Beni-Suef University Journal of Basic and Applied Sciences

RESEARCH

Open Access

Assessment of the protective and ameliorative impact of quercetin nanoparticles against neuronal damage induced in the hippocampus by acrolein

Samia M. Sanad[1], Safaa E. Nassar[1] and Reham Farouk[1*]

Abstract

Background The most frequent kind of dementia in the senior population is Alzheimer's disease (AD). Antioxidant quercetin has a low bioavailability. The bioavailability of quercetin nanoparticles was demonstrated to be higher. Acrolein is thought to be the strongest unsaturated aldehyde. Acrolein contributes to the propagation of oxidative damage and thus the aetiology of AD. This study aimed to investigate histopathological and ultrastructural changes that may arise in the hippocampus following acrolein treatment. Quercetin nanoparticles' ameliorative and protective effects on acrolein-induced neurotoxicity and oxidative stress were assessed.

Results We successfully synthesised quercetin nanoparticles with uniform size distributions and particle diameters in the range of 3.63–4.57 nm using transmission electron microscopy (TEM) and 3.7 nm using dynamic light scattering (DLS). Administration of acrolein was associated with histopathological alterations in the hippocampal structure, such as increased apoptotic neurones, dystrophic changes, neuronophagia, and atrophic ischaemia in cells, as well as marked damage to the ultrastructure of the hippocampus, which was obvious in shrunken pyramidal neurones with pyknotic nuclei and completely degenerated chromatin material, as well as in damaged astrocytes and microglial cells. Treatment with quercetin nanoparticles has been found to protect against and ameliorate the toxic effects and oxidative stress induced by acrolein in the hippocampus.

Conclusions This could pave the way for additional research in nanomedicine and a new line of therapeutic intervention in AD using nanoparticles such as quercetin nanoparticles.

Keywords Acrolein, Quercetin nanoparticles, Nanomedicine, Hippocampus, Ultrastructure, CA1, CA2, CA3, DG

1 Background

Alzheimer's disease (AD) is a deadly neurological illness marked by deteriorating cognitive function and memory [75]. The decrease in the functional activity of neurones in numerous brain regions, including those responsible for memory, emotional responses, learning, and behaviour, is a hallmark of AD. Two mechanisms that aid in the progression of AD are neurofibrillary tangled structures and plaques of amyloid, which are produced by deposits of beta-amyloid fragments (Aβ) and hyperphosphorylated tau proteins [57, 71].

Acrolein is α, β-unsaturated aldehyde with an unpleasant odour [42]. Acrolein in nature is mostly due to the partial combustion of organic particles, such as gasoline, coal, polymers, plastics, wood, and tobacco. Acrolein is generated when food is cooked or fried in solid or liquid oils [30]. Acrolein is also mostly present

*Correspondence:
Reham Farouk
reham.baiomy@zu.edu.eg
[1] Zoology Department, Faculty of Science, Zagazig University, Zagazig, Egypt

in foods, fruits, and beverages such as white bread, grapes, strawberries, and fried potatoes [24]. Endogenous acrolein synthesis takes place by lipid peroxidation (LPO) and the breakdown of polyunsaturated fatty acids through the amino acids and polyamines metabolism [36]. Tolerable Daily Intake (TDI) is estimated to be 7.5 mg/kg for acrolein [2]. Acrolein is regarded to be the most powerful electrophile of every α and β-unsaturated aldehydes. As a result, its great toxicity is due to its exceptionally strong reactivity towards biological nucleophiles [17]. Acrolein plays a function in the development of damage from oxidative stress [13]. Acrolein enhances tau protein phosphorylation, which is a significant pathologic characteristic of AD [33].

Among the flavonoids included in fruits and vegetables is quercetin such as white onion bulbs, lingonberries, cranberries, apples, cowpeas, fennel leaves, red onions, sweet potatoes, berries, citrus fruits, and tea [43]. Quercetin may prevent aggregation of the beta-amyloid peptide Aβ (1–42), notably dangerous compounds in the amyloid cascade, demonstrating its promise as a neuroprotective and anti-ageing medication [27]. In addition to its therapeutic benefits, water-insoluble quercetin has a limited oral bioavailability in blood [59]. Additionally, the blood–brain barrier, a solid barrier separating blood capillaries from interstitial fluid, is impervious to this water-insoluble polyphenolic molecule, which makes it extremely difficult to treat the central nervous system [33].

Due to its poor bioavailability and solubility, quercetin is rapidly degraded in the bloodstream, requiring larger doses and longer therapy periods [56]. Long-term use of quercetin, as well as excessive dosages, can have negative consequences [51]. Numerous synthetic or technological solutions, such as various medication delivery methods, have been devised to get around this restriction [12]. Quercetin and other natural and synthetic substances have been transported better thanks to nanoparticles [48]. The ability to administer drugs via several routes of administration, high carrier capacity, and biological system stability make nanoparticles an important drug delivery technology. These nanoparticle characteristics allow for increased medication bioavailability and decreased loss frequency [35].

To combat reactive oxygen species (ROS), quercetin nanoparticles can be used as effective antioxidants in the cytoplasm. Quercetin nanoparticles increase the bioavailability as well as solubility of quercetin [58]. They can penetrate numerous barriers, including the blood–brain barrier, owing to their unique physicochemical characteristics. Quercetin nanoparticles are frequently used in medical research [68].

Given their exceptional stability, high bioavailability, and fast ability to cross the blood–brain barrier, nanoparticles, particularly those made of hydrophobic substances like quercetin, have generated a great deal of attention in the treatment of AD. Consequently, due to quercetin's low bioavailability, low permeability, and hydrophobic nature, research on its therapeutic effects is still difficult. To boost oral bioavailability and brain permeability, the current study's goal was to produce quercetin nanoparticles using an antisolvent precipitation technique. It is important to investigate and assess the potential histopathological and ultrastructural alterations that could emerge from any potential toxic effects caused by acrolein, and the ameliorative and protective role of quercetin nanoparticles.

2 Methods

2.1 Experimental animals

Ninety male Rattus norvegicus, weighing 150–200 g and aged 10–12 weeks, were used. They came from Egypt's National Research Centre in Cairo. The rats were kept in polypropylene cages with wire-bar covers and pine shavings as bedding. They were also maintained under standard laboratory settings, including aeration, a room temperature of about 22–25˚c, and a 12-h light/dark cycle. The current experimental design was examined and authorised by the research ethical committee of Zagazig University, Egypt (approval number Zu-IACUC/1/F/306).

2.2 Chemicals

Chemicals used were of the highest commercial grade. Quercetin (>98% pure) was purchased from Fine-Chem Limited (SDFCL), Industrial Estate, 248, Worli Road, Mumbai, Maharashtra, India. Acrolein (99% pure) was obtained from Pharmachem Fine Chemicals for Research and Industry, Mumbai, India.

2.3 Preparation of Quercetin nanoparticles

The previously mentioned precipitation process was used to create quercetin nanoparticles with a few changes [1]. As the organic phase, quercetin (5 mg) was dispersed in ethanol (1 ml) in the water bath at 40 °C. The resulting solution was added at a concentration of 1:40 to deionised water (antisolvent), which was then agitated magnetically at 3000 rpm for 10 min. A fixed flow rate of 10 ml/min was used to add the prepared solution to the water. A water bath set at 60 °C was used to evaporate all the ethanol. The purification and vacuum drying of quercetin nanoparticles were done.

2.4 Quercetin nanoparticles characterisation

2.4.1 Analysis of particle size

Using a Zetasizer Nano ZS (Malvern Instruments Ltd., Malvern, UK), DLS was utilised to assess particle size. Quercetin nanoparticles were diluted with ethanol to ensure the signal intensity was suitable for the device. With ethanol (viscosity (cp) of 0.1000) at 25°C, the nanoparticles were diluted, and the intensity of the scattered light was assessed at an angle of scattering of 173° to the direction of the incident wave. The readings were made in triplicate, and the polydispersity ranged from 0 to 1.

2.4.2 1.1.1 Morphology of the particles

The shape of the quercetin nanoparticles was examined using TEM. The samples were placed on a copper grid with a mesh size of 300 µm and examined using a JEOL JEM 1400 TEM (Tokyo). Uranyl acetate (10 mL) was used as a contrast agent for 10 s.

2.5 1.1 Experimental design

Following adaptation for two weeks, the rats were separated into six groups of 15 rats each, as follows: Control group: rats received 1 ml of distilled water for 30 days. Acrolein-treated group: rats received acrolein (3 mg/kg) [18] for 30 days. Quercetin nanoparticle-treated group: For 30 days, the rats received quercetin nanoparticles (30 mg/kg) [70]. Ameliorative group: rats received acrolein (3 mg/kg) and quercetin nanoparticles (30 mg/kg) at the same time for 30 days. Protective group: rats received a dose of quercetin nanoparticles (30 mg/kg) for 30 days and then acrolein (3 mg/kg) for another 30 days. Recovery group: The rats received acrolein (3 mg/kg) for 30 days, after which they were left to recover for 30 days without any other treatment.

2.6 1.1 Necropsy schedule

At the end of the experimental period, the animals were sacrificed 24 h after the last dose. The skulls of all the rats were opened. The hippocampus was made visible by removing the brains and splitting them into two hemispheres. Both the control and treated rats' hippocampi were sliced to the same thickness and put in the same fixative.

2.7 2.7 Histological technique

2.7.1 2.7.1 For histological analysis

Following decapitation, samples from the experimental groups immediately underwent fixation in 10% neutral buffered formalin for 24 h, washed in tap water, put in 70% ethanol, dehydrated in an ascending series of ethanol solutions, cleaned in xylene, and lastly inserted into paraffin wax. Serial slices with a thickness of around 5 µm were cut using a rotary microtome (Leica, Model Rm 2125, Germany), and they were then stained [78] to demonstrate the histological structure.

2.7.2 Morphometric analysis:

To show alterations in various parts of the hippocampus, light microscopy was used. Intact hippocampal neurones, normal pyramidal cells, and granular cells were manually counted from five randomly chosen hematoxylin and eosin-stained sections from five different animals from both control and treated groups using a light microscope under a 40X objective. The measured histometric factors were the cell body diameter of the pyramidal and granular cells and the granular layer and pyramidal layer thickness [70].

2.7.3 Semi-quantitative scoring of the neuronal histopathological lesions

The degree of damage to brain tissue was assessed using a semi-quantitative evaluation method that examined five randomly selected fields from each section. Semi-quantitative ratings of the degree of neuronal injury in the hippocampus were given. The tissue sections were analysed for cellular oedema, ischaemia damage, Malacia, gliosis, and the extent of the lesions. According to the percentage of affected tissue, the degree of severity of lesions was scored and graded as follows: none (-) = 0%, indicating no detectable lesions; mild lesions (+) = 5–25% of the approved field; moderate lesions (++) = 25–50% of the approved field; severe focal lesions (+++) = 50–80% of the approved field; and severe diffuse lesions (++++) = 80–100% of the approved field [26].

2.8 1.1 Ultrastructural studies

Hippocampal tissue was removed and chopped into tiny (1 mm3) pieces. The specimens were fixed in 2.5% glutaraldehyde. Glass knives were used to cut semi-thin slices (0.5 mm) with a microtome (Power Tome XL, USA). Ultrathin slices (80–90 nm) were prepared using a diamond diatoms knife on an ultramicrotome (Power Tome XL, USA). The slices were inspected and photographed using a Jeol 100S TEM (Joel-JEM-100 CXII; Joel, Tokyo, Japan).

2.9 1.1 Statistical analysis

The data are shown as the mean ± SD of the various treatment groups. ANOVA was used to examine the differences between the mean values, followed by the Student's t test applying the Minitab 12 computer programme (Minitab Inc., State College, PA, USA), and a p-value of $p < 0.05$ was deemed statistically significant.

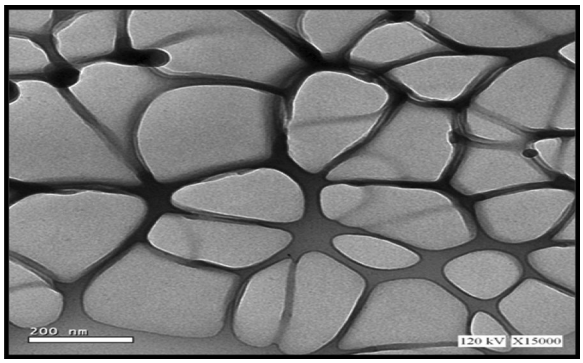

Fig. 1 TEM image of original quercetin

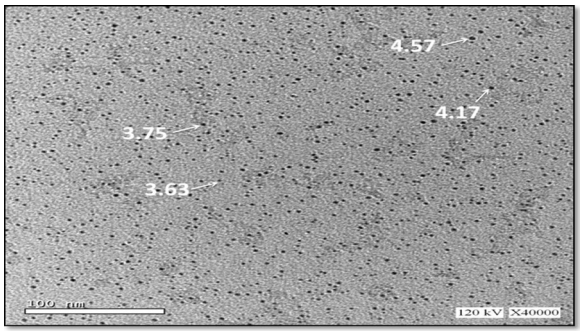

Fig. 2 TEM image of quercetin nanoparticles. The nanoparticles size was about 3.63–4.57 nm

3 Results

3.1 Preparation and characterisation of quercetin nanoparticles

Quercetin nanoparticles were produced, and their structural and biological characteristics were examined. Pure quercetin was used as the precursor for the quercetin nanoparticles synthesis. The original quercetin powder (Fig. 1) contained particles with a lack of uniformity in size that were significantly larger than the quercetin nanoparticles. In contrast, quercetin nanoparticles prepared by the precipitation technique had a more uniform particle size and less crystallinity. TEM revealed that the quercetin nanoparticles were morphologically spherical with a uniform size distribution, as shown in Fig. 2. The diameter of the quercetin nanoparticles at a solvent/antisolvent volume ratio of 1:40, stirring speed of 3000 rpm, and quercetin concentration of 5 mg/ml was in the range of 3.63–4.57 nm, as indicated in Fig. 2.

DLS data, the most widely used nanoparticle characterisation method, revealed that the ethanolic dispersion of quercetin nanoparticles resulted in the formation of nanoparticles with an average hydrodynamic diameter of 3.7 nm, as indicated in Fig. 3. This result is consistent with that obtained from the TEM images.

3.2 Histopathological studies

Examination of sections from the hippocampus of the normal control group showed normal organisation of the hippocampal formation. It was made up of three parts: the hippocampal proper (Cornu Ammonis), dentate gyrus (DG), and subiculum (S). The hippocampus

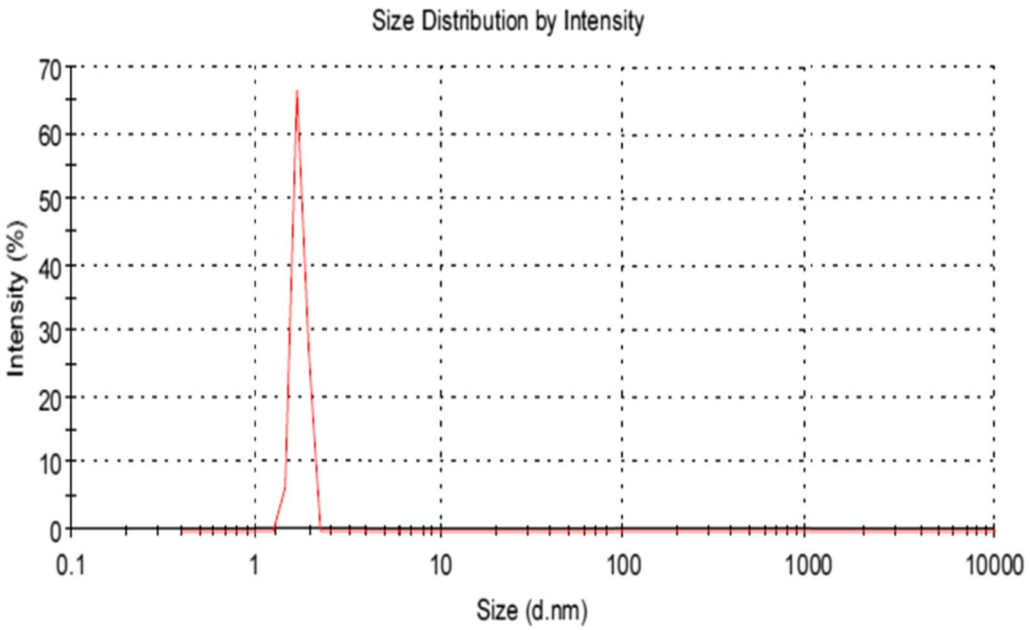

Fig. 3 DLS of the quercetin nanoparticles

proper was depicted as a C-shaped that was segmented into four separate areas known as the Cornu Ammonis (CA1, CA2, CA3, and CA4). The DG is a curved trilayered cortex that forms a cap-like structure. The DG is observed around CA4 with its upper and lower limbs. The S is the transition region between the CA1 and the entorhinal region. It is composed of three parts: the proper subiculum, presubiculum, and parasubiculum as shown in Fig. 4.

The proper hippocampal cortex is composed of three basic layers: the stratum radiatum, stratum pyramidale, and stratum oriens. The stratum pyramidale is recognised the middle dark zone. It contains primary hippocampal excitatory neurones. This layer also contained a few interneurons. In CA1, the stratum pyramidale is composed of large pyramidal neurones organised into 4–6 layers of cells. The nuclei appeared large and oval to spherical with conspicuous nucleoli, as shown in Fig. 5a. In CA2, the stratum pyramidale appeared smaller than that in CA1 and was organised into 3–4 cell layers, as indicated in Fig. 6a. In CA3, the stratum pyramidale appeared larger and was composed of two to five cell layers with a thick, voluminous axon hillock, as shown in Fig. 7a. The DG has three layers: the molecular, granular, and polymorphic. Its molecular layer is adjacent to the hippocampus. The DG is characterised by its granular layer, which is composed of densely packed small-to-medium-sized granular cells that form a U-shaped configuration that opens towards the fimbria. Granule cell axons pass through the polymorphic layer on their way to pyramidal cell dendrites in the hippocampus proper (CA3). The polymorphic layer contained several cell types, including pyramidal neurones as shown in Fig. 8a.

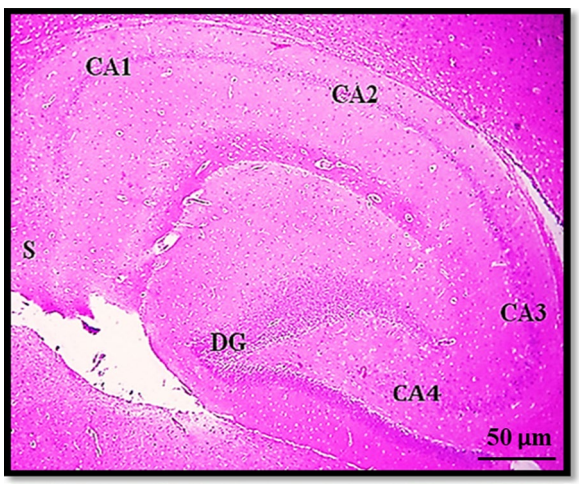

Fig. 4 Section in the hippocampus of a control rat showing normal organisation of hippocampus formation. Cornu ammonis 1 (CA1), Cornu ammonis 2 (CA2), Cornu ammonis 3 (CA3), Cornu ammonis 4 (CA4), dentate gyrus (DG), and subiculum (S). (X40)

In the acrolein-treated group, the hippocampal formation revealed distinct histological abnormalities affecting CA1, CA2, CA3, and DG. CA1 exhibited a significant decrease in the thickness of the stratum pyramidal layer, with increased apoptotic neurones accompanied by dystrophic alterations in the form of shrunken hyperchromatic and irregular with chromatolysis, as shown in Fig. 5b. CA2 showed a significant reduction in the stratum pyramidal layer thickness, with severe atrophic ischaemic injury of the stratum pyramidal layer neuronal cells and increased apoptotic neurones, as indicated in Fig. 6b. CA3 revealed a reduced thickness of the stratum pyramidale as well as a significant degree of atrophic ischaemic injury of the stratum pyramidale layer's neuronal cells, which was accompanied by marked neuronophagia, as indicated in Fig. 7b. Acrolein-induced atrophic ischaemia injury in the granular cells of the granular layer in the hippocampal DG, as shown in Fig. 8b.

Examination of sections from the hippocampal regions (CA1, CA2, CA3, and DG) of the quercetin nanoparticle-treated group revealed that quercetin nanoparticles significantly preserved the cellular structure to a high extent. The hippocampal CA1, CA2, and CA3 sections showed normal neuronal cells within the stratum pyramidale layer. The thickness of the stratum pyramidale layer appears normal, as shown in Figs. 5c, 6c, and 7c, respectively. The DG section revealed typical, densely packed, tiny granular cells. The thickness of the granular layer increases in the DG region, as shown in Fig. 8c. Quercetin nanoparticles had the overall impact of preserving the normal cellular morphology of hippocampal cells.

Different hippocampal locations in the ameliorative group showed marked improvements in histological patterns. The sections in CA1, CA2, and CA3 demonstrated a reduction in the ischaemic neuronal injury of the neuronal cells of the stratum pyramidale layer, as well as an improvement in the stratum pyramidale layer thickness, as shown in Figs. 5d, 6d, 7d, respectively. The DG hippocampal sections of the ameliorative group showed a reduction in ischaemia neuronal damage within the granular cells of the granular layer (Fig. 8d).

The histological structure of the hippocampus in the protective group appeared to be well-protected from injury resulting from acrolein treatment. As shown in Figs. 5e, 6e, and 7e, the sections from the protective group in CA1, CA2, and CA3 of the hippocampus showed a significant decrease in neuronal injury of the neuronal cells of the stratum pyramidale layer and a marked enhancement in the thickness of the stratum pyramidale layer. As shown in Fig. 8e, DG hippocampal

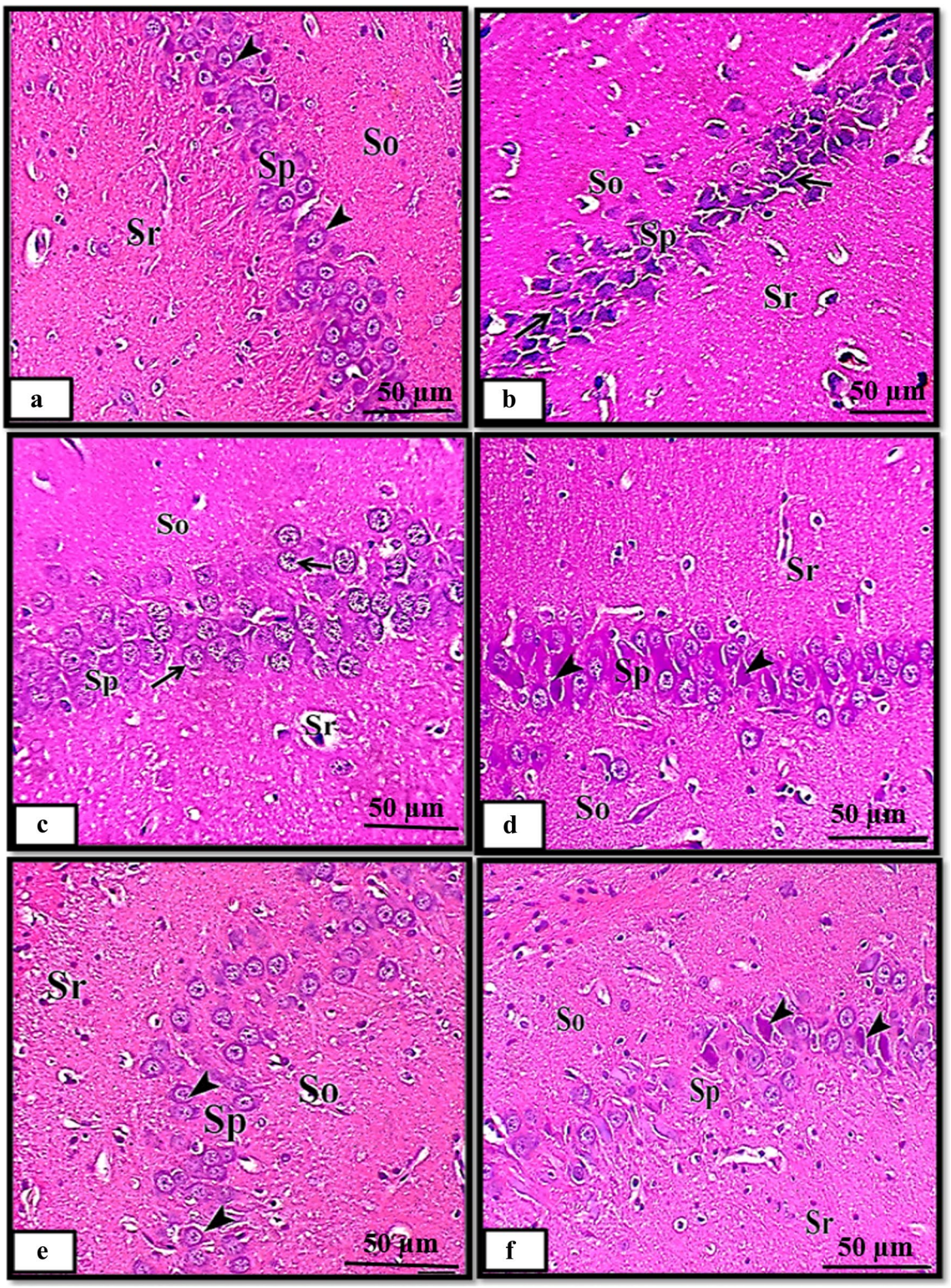

Fig. 5 Photomicrograph in CA1 of the hippocampus **a** Control group showing a normal structure of CA1. **b** Acrolein-treated group showing increased apoptotic neurones with dystrophic changes in the form of shrunken hyperchromatic, chromatolysis (arrows). **c** Quercetin nanoparticle-treated group showing normal neuronal cells (arrows). **d** Ameliorative group showing a decrease in ischaemic neuronal injury of neuronal cells (arrowheads indicate atrophic cells). **e** Protective group showing a marked decrease in neuronal injury of the neuronal cells (arrowheads). **f** Recovery group showing a minor decrease in ischaemic neuronal injury of neuronal cells (arrowheads). (Sr: stratum radiatum, So: stratum oriens, Sp: stratum pyramidale). (X400)

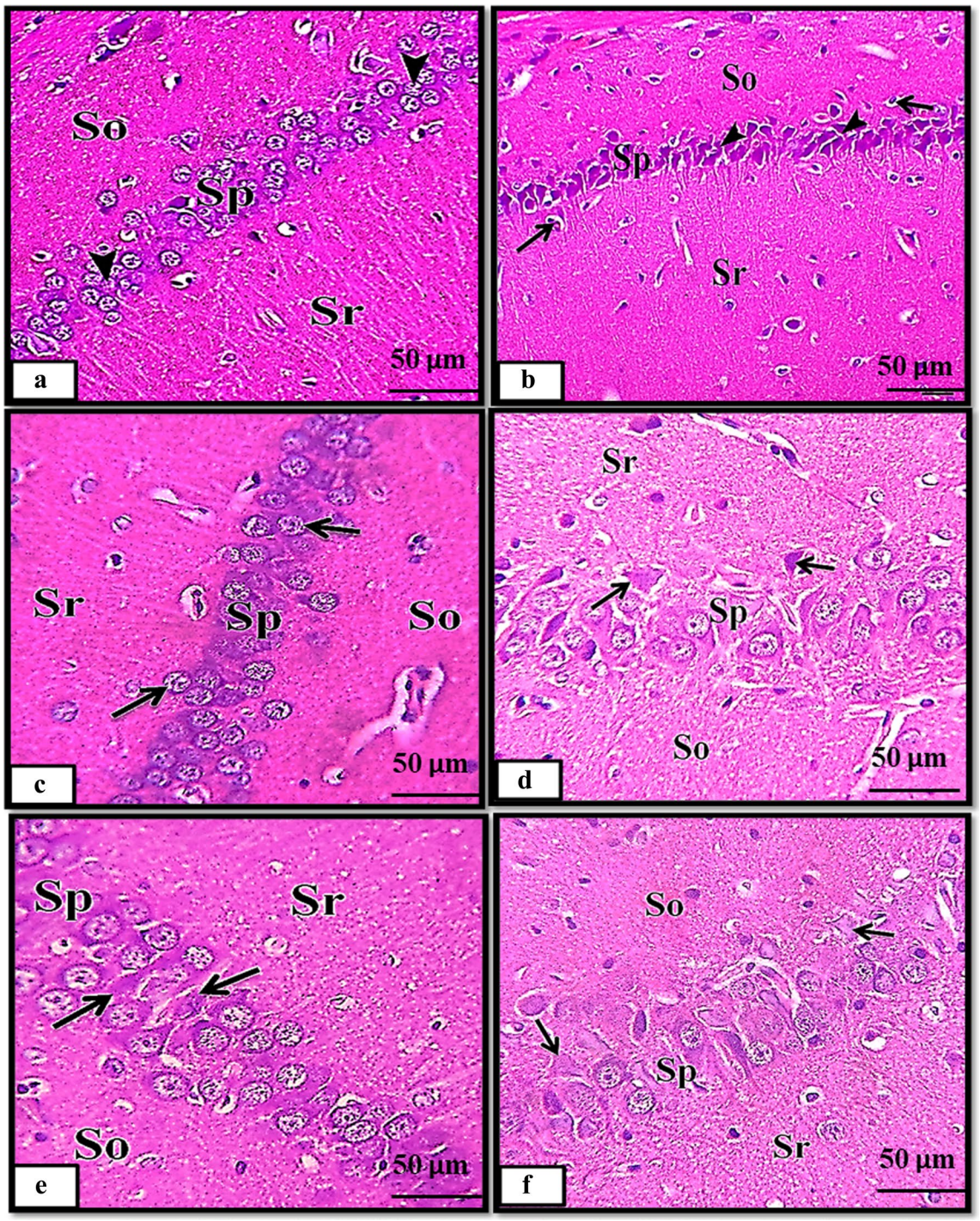

Fig. 6 Photomicrograph in CA2 of the hippocampus **a** Control group showing a normal structure of CA2 with normal pyramidal neurones (arrowheads). **b** Acrolein-treated group showing a significantly decreased thickness of the Sp layer, with a severe degree of atrophic ischaemic injury of the neuronal cells of the Sp layer (arrowheads) and increased apoptotic neurones (arrows). **c** Quercetin nanoparticle-treated group showing normal thickness of the Sp layer with normal neurones (arrows). **d** Ameliorative group showing a reduction in ischaemic neuronal injury in the neuronal cells of the Sp layer (arrows indicate the atrophic cells) with significantly increased Sp layer thickness. **e** Protective group showing neuronal cells of the Sp layer experienced a significant reduction in neuronal injury (arrows indicate atrophic cells). **f** Recovery group showing a very slight decrease in ischaemic neuronal injury of the neuronal cells of the Sp layer (arrows) (Sr: stratum radiatum, So: stratum oriens, Sp: stratum pyramidale). (X400)

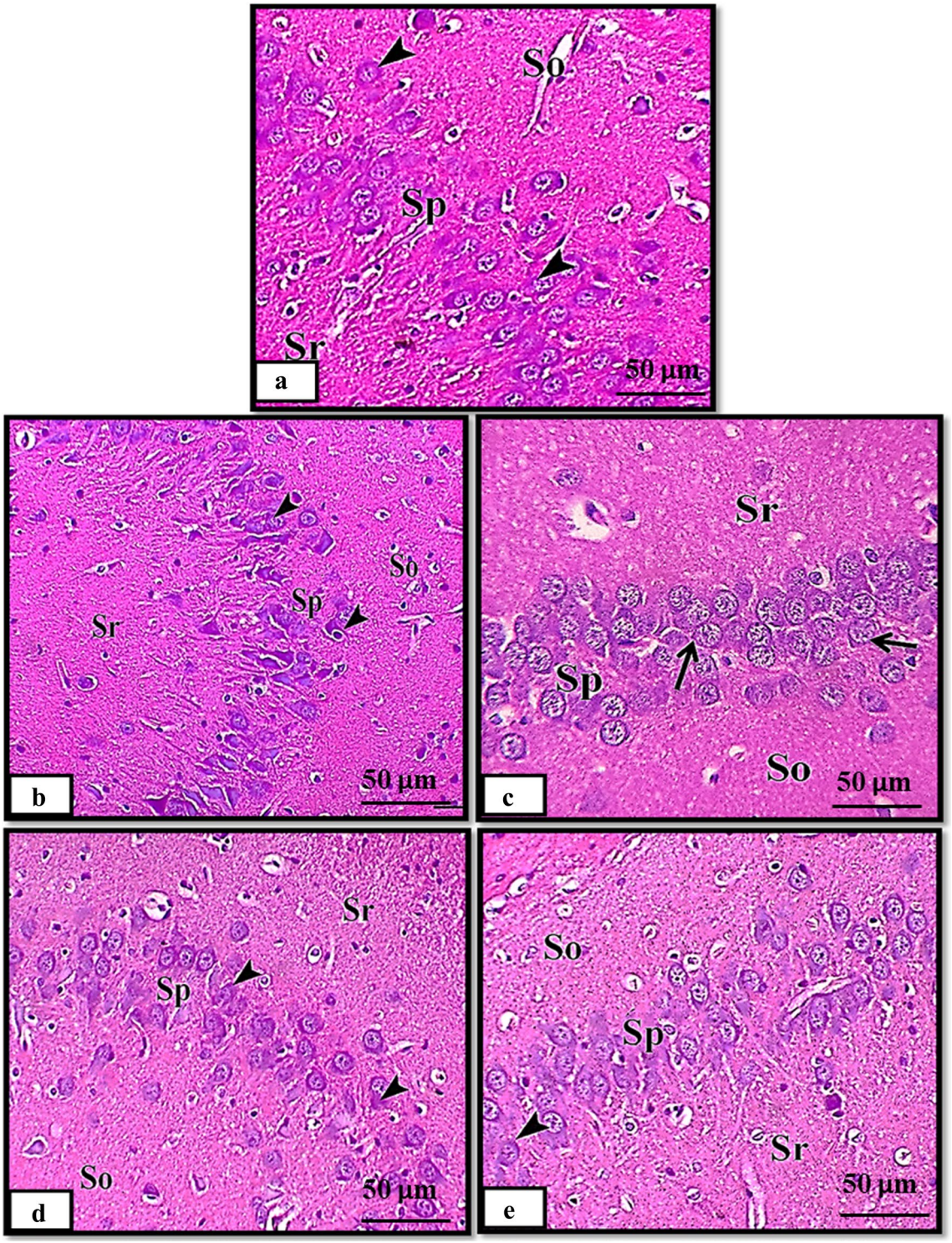

Fig. 7 Photomicrograph in CA3 of the hippocampus **a** Control group showing a normal structure of CA3 with normal pyramidal neurones (arrowheads). **b** Acrolein-treated group showing a reduction in the thickness of the Sp layer as well as a severe degree of atrophic ischaemic injury of the neuronal cells of the Sp layer associated with marked neuronophagia (arrowheads). **c** Quercetin nanoparticle-treated group showing normal thickness of the Sp layer and normal large neurones (arrows). **d** Ameliorative group showing a decrease in ischaemic and lytic changes within the neuronal cells of the Sp layer (arrowheads) with significantly improved Sp layer thickness. **e** Protective group showing that the neuronal cells of the Sp layer appear normal (arrowhead), as does the thickness of the Sp layer. (Sr: stratum radiatum, So: stratum oriens, Sp: stratum pyramidale). (X400)

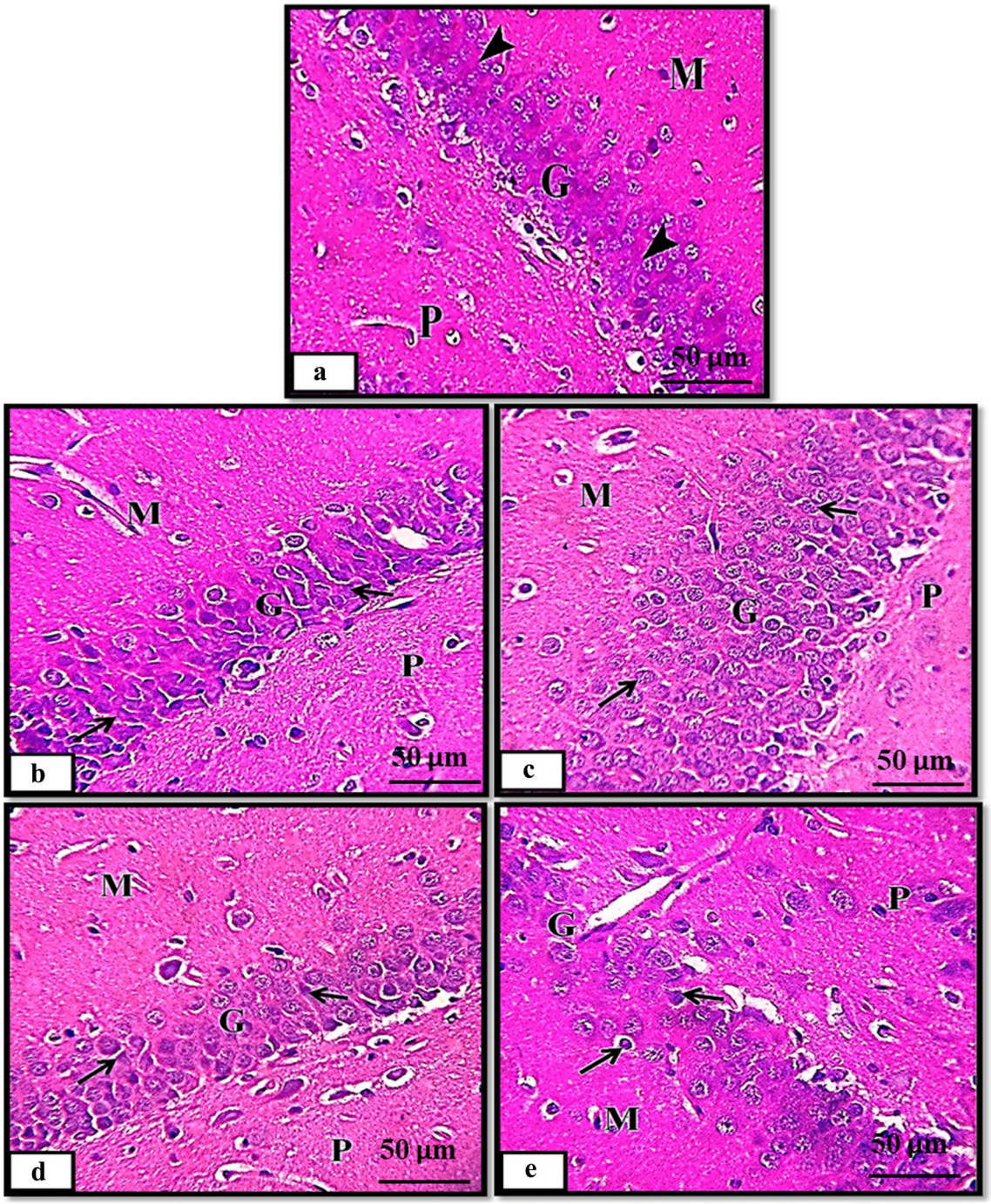

Fig. 8 Photomicrograph in the DG of the hippocampus **a** Control group showing a normal structure of DG and normal densely packed small granular cells (arrowheads). **b** Acrolein-treated group showing atrophic ischaemic injury of the granular cells of the granular layer (arrows). **c** Quercetin nanoparticle-treated group showing normal, densely packed, and small granular cells (arrows). An increase in the thickness of the granular layer was observed. **d** Ameliorative group showing a decrease in ischaemic neuronal injury within granular cells of the granular layer (arrows indicate atrophic cells). **e** Protective group showing a significant decline in atrophic ischaemic neuronal injury within the granular cells of the granular layer (arrows represent atrophic cells). (M: molecular layer, P: polymorphic layer, G: granular layer). (X400)

sections of the protective group showed a significant reduction in atrophic ischaemic neuronal injury within the granular cells of the granular layer. In the recovery group, hippocampal CA1 and CA2 sections showed a slight reduction in atrophic ischaemic injury and neuronophagia of the neuronal cells of the stratum pyramidale layer, as shown in Figs. 5f and 6f.

3.3 Morphometric analysis for the hippocampus

3.3.1 Pyramidal and granular neurones number

A significant decrease was observed in the normal pyramidal neurones number in the CA1, CA2, and CA3 regions, and a decrease in the number of normal granular neurones in the DG region in the acrolein-treated group as shown in Fig. 9. The number of these cells in the ameliorative and protective groups was significantly higher than in the acrolein-treated group. There was no significant difference between the recovery and acrolein-treated groups in the normal pyramidal neurones number and the number of normal granular neurones.

3.3.2 The cell body diameters of pyramidal and granular cells

The cell body diameter of pyramidal cells in the CA1, CA2, and CA3 regions and granular cells in the DG region in rats that received acrolein decreased significantly. Following treatment with quercetin nanoparticles, the cell body diameter of the pyramidal and granular cells was significantly increased in the ameliorative and protective groups, whereas in the recovery group, the size of the cell body of these cells was slightly increased when compared to that of the acrolein-treated group (Table 1).

3.3.3 The thickness of the pyramidal layer in the CA1, CA2, and CA3 regions and the granular layer in the DG region of the hippocampus:

Treatment of rats with acrolein caused hippocampal layer atrophy. Acrolein reduced the pyramidal layer thickness in the CA1, CA2, and CA3 regions and the granular layer. Treatment of rats with quercetin nanoparticles significantly increased the pyramidal layer thickness and the granular layer in the ameliorative group. The thickness of

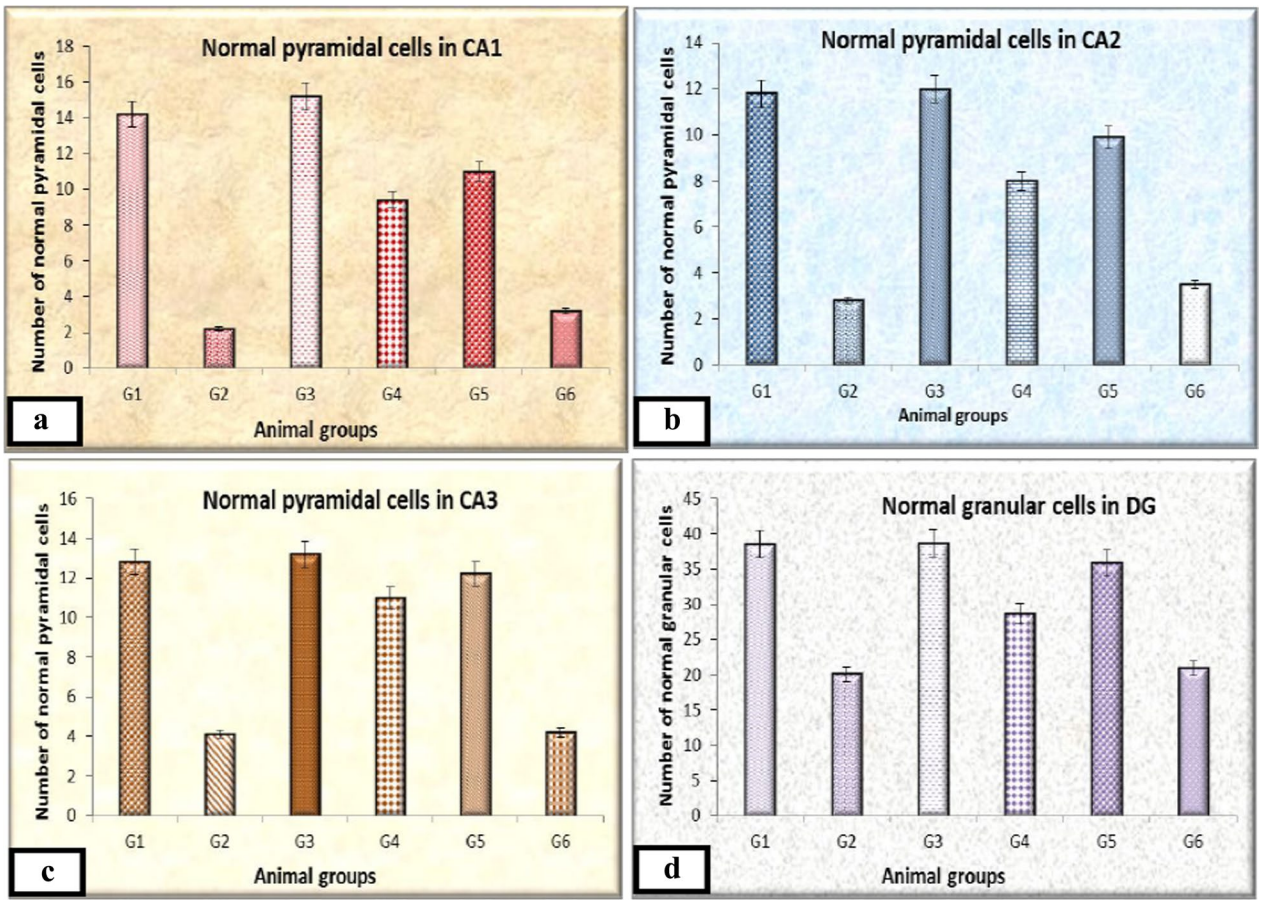

Fig. 9 Number of normal pyramidal cells in CA1, CA2, and CA3, and number of normal granular cells in the DG from the studied groups (G1: Control group, G2: acrolein-treated group, G3: quercetin nanoparticle-treated group, G4: ameliorative group, G5: protective group, G6: recovery group). Data are expressed as (mean ± SD), ($P < 0.05$)

the pyramidal layer and the granular layer in the protective group significantly increased in thickness. The thickness of these layers was slightly higher in the recovery group than in the acrolein-treated group (Table 2).

3.4 Semi-quantitative scoring of neuronal histopathological lesions in the hippocampus

The semi-quantitative scoring of the reported lesions showed a significant increase in hippocampal tissue injury in the acrolein-treated group. Semi-quantitative scoring of neuronal histopathological lesions in the acrolein-treated group indicated severe cellular oedema, ischaemic injury, malacia, gliosis, and the extent of the lesions. Rats that received quercetin nanoparticles in the ameliorative and protective groups significantly avoided hippocampal tissue damage compared to acrolein-treated rats (Table 3). In the ameliorative group, the semi-quantitative scoring indicated mild cellular oedema, gliosis, and extent of lesions, moderate ischaemic injury, and no detectable malacia, while in the protective group, there was no cellular oedema, malacia, gliosis, and extent of lesions and revealed mild ischaemic injury. In the recovery group, semi-quantitative scoring indicated severe cellular oedema, ischaemic injury, and the extent of lesions, as well as moderate malacia and gliosis.

Table 1 Cell body diameter (μm) of pyramidal cells in the hippocampal CA1, CA2, and CA3 regions and cell body diameter (μm) of granular cells in the DG region in the different treatment groups. Data are expressed as (mean ± SD), ($P < 0.05$)

Groups	Cell body diameter (μm) of pyramidal cells			Cell body diameter (μm) of granular cells
	CA1	CA2	CA3	
Control group	24.22 ± 0.28	22.25 ± 0.43	24.87 ± 1.02	13.21 ± 0.61
Acrolein-treated group	18.01 ± 0.66	10.12 ± 0.01	20.55 ± 0.27	9.25 ± 0.73
Quercetin nanoparticle- treated group	24.62 ± 0.52	22.75 ± 0.53	24.92 ± 0.97	13.22 ± 0.87
Ameliorative group	21.12 ± 0.23	20.86 ± 0.57	23.61 ± 0.92	12.64 ± 1.04
Protective group	23.22 ± 0.84	21.72 ± 0.92	23.96 ± 0.44	12.91 ± 0.26
Recovery group	20.32 ± 0.45	18.22 ± 0.01	22.21 ± 0.38	10.37 ± 0.02

Table 2 The thickness (μm) of the pyramidal layer in hippocampal CA1, CA2, and CA3 regions and the thickness (μm) of the granular layer in the DG region in the different treatment groups. Data are expressed as (mean ± SD), ($P < 0.05$)

Groups	Thickness (μm) of the pyramidal cells			Thickness (μm) of granular cells
	CA1	CA2	CA3	
Control group	70.72 ± 1.58	68.43 ± 1.52	73.67 ± 1.75	72.58 ± 1.42
Acrolein-treated group	45.76 ± 1.57	40.02 ± 1.38	52.28 ± 1.74	68.16 ± 1.38
Quercetin nanoparticle-treated group	70.83 ± 2.21	69.5 ± 1.14	73.66 ± 2.21	74.57 ± 2.45
Ameliorative group	68.01 ± 1.65	66.25 ± 2.63	71.51 ± 2.13	71.34 ± 2.15
Protective group	70.16 + 1.37	68.13 ± 1.83	72.21 ± 1.03	72.37 ± 2.32
Recovery group	48.14 ± 1.02	46.81 ± 1.04	54.47 ± 2.13	69.25 ± 1.84

Table 3 Semi-quantitative scoring of neuronal histopathological lesions in the hippocampus in the different treatment groups

Groups	Cellular oedema	Ischaemic injury	Malacia	Gliosis	Extent of lesions
Control group	-	-	-	-	-
Acrolein-treated group	+ + +	+ + + +	+ +	+ + +	+ + +
Quercetin nanoparticle-treated group	-	-	-	-	-
Ameliorative group	+	+ +	-	+	+
Protective group	-	+	-	-	-
Recovery group	+ + +	+ + +	+ +	+ +	+ + +

(-) denotes no detectable lesions; (+) mild lesions; (++) moderate lesions; (+++) severe focal lesions; (++++) severe diffuse lesions

3.5 Ultrastructural alterations

3.5.1 The pyramidal neurons

Examination of ultrathin sections from the control group hippocampus indicated the presence of healthy pyramidal neurones with large, rounded nuclei and dispersed chromatin. The cytoplasm had a well-developed rough endoplasmic reticulum, intact elongated or spherical mitochondria, well-developed Golgi apparatus, and primary lysosomes, as shown in Fig. 10a. In the acrolein-treated group, pyramidal neurons showed a shrunken electron-dense cytoplasm and completely damaged neurones with an empty vacuolar structure, as shown in Fig. 10b. Pyramidal neurones also show a pyknotic nucleus, completely degenerated chromatin material, and deformation of the nuclear membrane. The rough endoplasmic reticulum, mitochondria, Golgi apparatus, and lysosomes are completely damaged. Ultrathin hippocampal sections examined from rats treated with quercetin nanoparticles showed a normal ultrastructural structure of pyramidal neurones, as shown in Fig. 10c. In the ameliorative and protective groups (Fig. 10d, e, respectively), the pyramidal neurones had significantly improved ultrastructures compared to the acrolein-treated group. The rough endoplasmic reticulum, mitochondria, and primary lysosomes appeared to be normal. The nucleus appeared normal, with dispersed chromatin, but an irregular nuclear membrane. Small cytoplasmic vacuoles were observed in the ameliorative group. Pyramidal neurones in the recovery group exhibited no improvement in ultrastructure compared to the acrolein-treated group, as demonstrated in Fig. 10f.

3.5.2 The astrocytes

As illustrated in Fig. 11a, the control group exhibited normal astrocytes with oval or round nuclei surrounded by pale cytoplasm. Heterochromatin is evenly distributed beneath the inner nuclear envelope. Numerous organelles occupy the cytoplasm. In the acrolein-treated group, degenerative alterations in the astrocytes were exacerbated. A swollen nucleus and slight heterochromatin clumping at the nuclear periphery were observed. One notably injured astrocyte cytoplasm was almost empty, with dispersed residual damaged cellular organelles such as ruptured mitochondrial cristae with large vacuoles as shown in Fig. 11b. In the quercetin nanoparticle-treated group, astrocytes revealed a normal cell with a round heterochromatic nucleus, which was regular in shape and surrounded by a scanty cytoplasm when compared with the control group, as shown in Fig. 11c. In the ameliorative and protective groups, quercetin nanoparticles exerted a beneficial effect on the ultrastructure of astrocytes in the hippocampus. These astrocytes showed slight abnormalities compared with those in the control group. The nucleus appeared normal, surrounded by a scant cytoplasm, but had an irregular cell membrane. Heterochromatin was evenly distributed beneath the inner nuclear envelope. Several organelles were in the normal condition (Fig. 11d, e). In the hippocampus of the recovery group, there was a slight improvement in the ultrastructure of astrocytes compared to the acrolein-treated group, as indicated in Fig. 11f.

3.5.3 The microglia

The control group had typical microglia with dark elongated nuclei and clumped chromatin (Fig. 12a). The cytoplasm appeared dark and included the endoplasmic reticulum, with long stretches. In the acrolein-treated group, microglia displayed significant degenerative alterations. These degenerative alterations include shrunken and completely damaged microglia with pyknotic nuclei. The chromatin material and nucleoli were also completely degenerated and the nuclear membrane became distorted, as shown in Fig. 12b. The ultrastructure of the microglial cells in the quercetin nanoparticle-treated group showed a normal, dark, elongated nucleus with clumped chromatin. The cytoplasm appeared dark and had long stretches of endoplasmic reticulum, as shown in Fig. 12c. Quercetin nanoparticles have been proven to have a significant positive effect on the ultrastructure of hippocampal microglia in ameliorative and protective groups. As indicated in Fig. 12d, e, the nucleus appeared normal with clumped chromatin and a dark cytoplasm. A modest improvement in the ultrastructure of microglia in the hippocampus of the recovery group was observed compared to that in the acrolein-treated group. An irregular nucleus with nuclear chromatin condensation and a dark cytoplasm was observed, as shown in Fig. 12f.

3.5.4 Myelin sheath

Normal myelin sheaths in the control group appeared thick, extremely electron-dense, and firmly wrapped around the axonal cytoplasmic membranes. The myelinated axons had smooth, regular contours, as shown in Fig. 13a. Several types of myelin defects appeared in the acrolein-treated group (Fig. 13b). In this case, the myelin sheath showed areas of thinning with focal interruption. Some myelin sheaths were entirely damaged. The axoplasm exhibited vacuolation. In the quercetin nanoparticle-treated group, the ultrastructure of the myelin sheath in the hippocampus appeared normal. As depicted in Fig. 13c, it is apparent that a typical myelin sheath is thick, electron-dense, and tightly wrapped around axonal cytoplasmic membranes. Axons that have been myelinated have smooth and consistent shapes. In both the ameliorative and protective groups, quercetin nanoparticles were shown to have a significant beneficial effect on

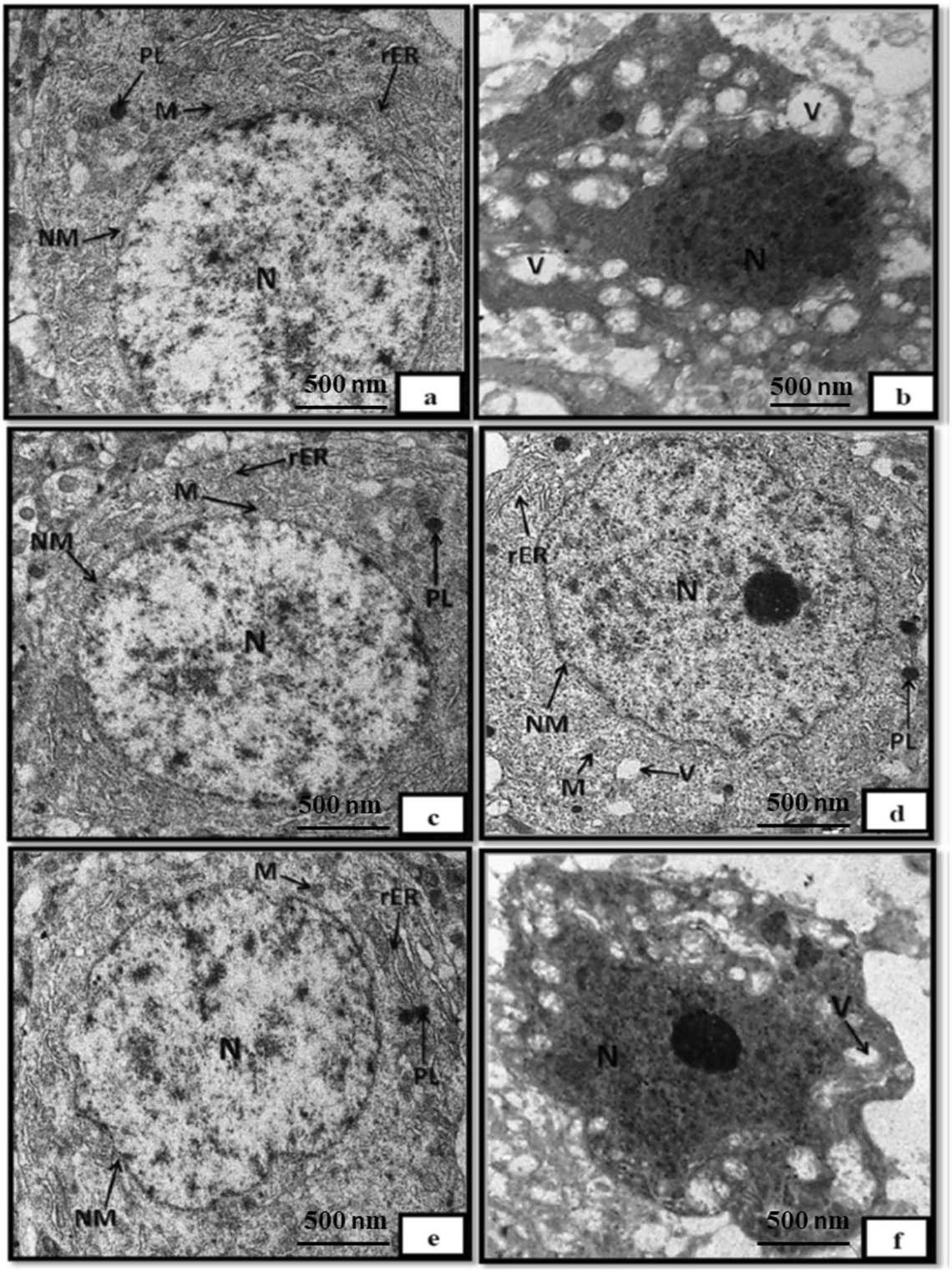

Fig. 10 Electron micrograph of pyramidal neurones **a** Control group showing normal pyramidal neurones. **b** Acrolein-treated group showing a shrunken and completely damaged neuron with an empty vacuolar structure (v), pyknotic nucleus, degraded chromatin, completely degenerated organelles, and NM deformation. **c** Quercetin nanoparticle-treated group showing normal pyramidal neurones. **d** Ameliorative group showing N with irregular NM and small cytoplasmic vacuoles. e) Protective group showing N with irregular NM, well-developed rER, spherical M, and PL. **f** Recovery group revealed a severely injured neuron with an empty vacuolar structure, NM deformation, and a pyknotic nucleus. (N, nucleus; NM, nuclear membrane; rER, rough endoplasmic reticulum; M, mitochondria; PL, primary lysosomes; V, vacuolar structure). X 10000

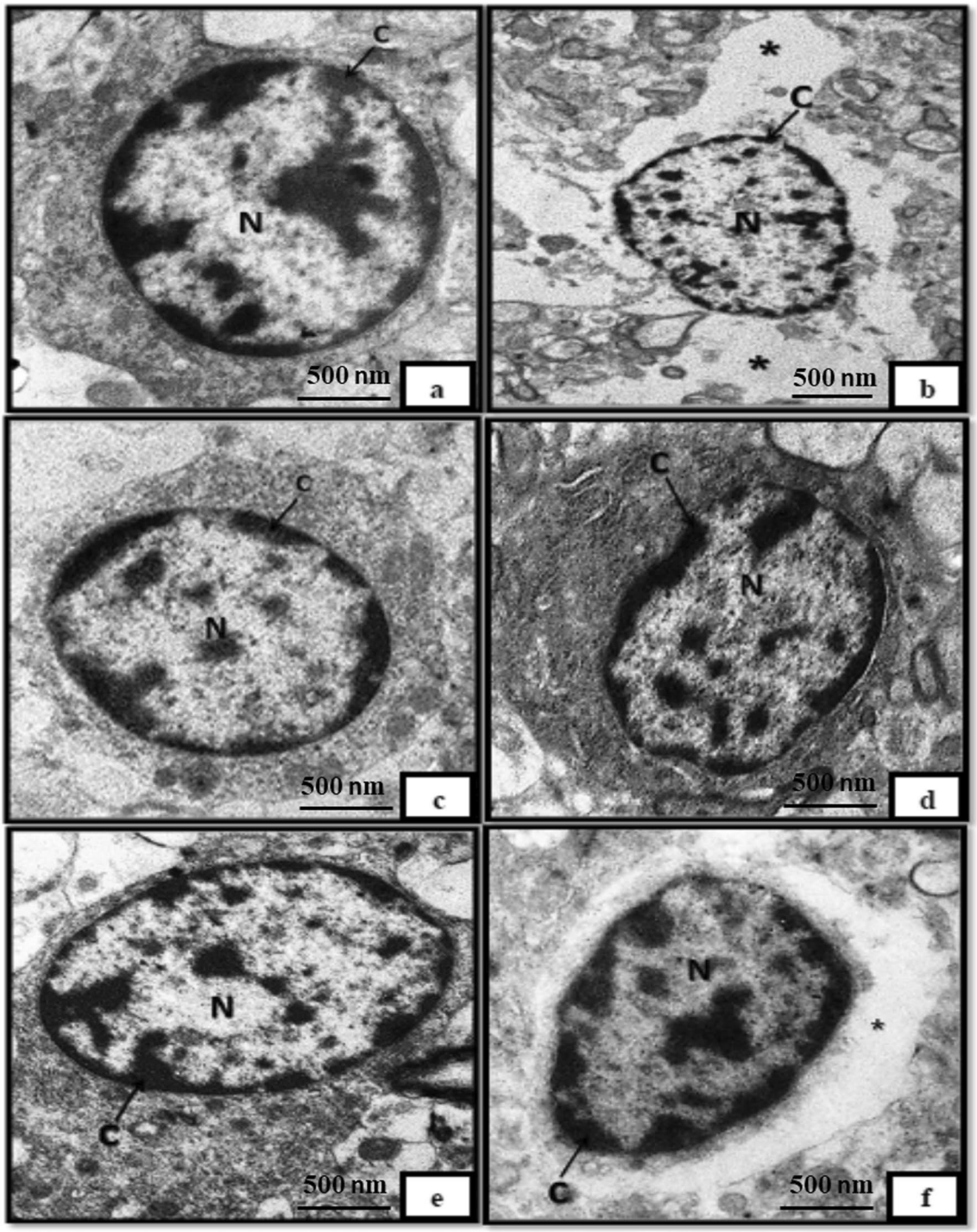

Fig. 11 Electron micrograph of the astrocytes **a** Control group showing a round heterochromatic nucleus that is usually regular in shape and surrounded by scanty cytoplasm. **b** Acrolein-treated group showing swollen N with slight heterochromatin clumping at the nuclear periphery and severely damaged cytoplasm with scattered residual damaged cellular organelles. **c** Quercetin nanoparticle-treated group showing normal astrocytes. **d** Ameliorative group showing normal nuclei. Heterochromatin spread uniformly underneath the inner nuclear envelope. **e** Protective group showing a normal heterochromatin nucleus surrounded by a scant cytoplasm. **f** Recovery group showing a slightly swollen N. Cytoplasm with scattered residual cellular organelles. (N, nucleus; C, heterochromatin material; black star, clear area and loss of organelles). X 15000

the ultrastructure of the hippocampal myelin sheath. This was evident by the preservation of the myelin sheath, except for a very few axons. Most of the myelin sheaths were restored compared with the acrolein-treated group, as indicated in Fig. 13d, e. The ultrastructure of the myelin sheath in the hippocampus of the recovery group was higher than that in the acrolein-treated group, as shown in Fig. 13f.

4 Discussion

Alzheimer's is a neurological illness that destroys brain cells, causing memory deprivation and severe mental and behavioural impairments [41, 54]. The number of patients afflicted by AD is rapidly growing owing to the ageing human population; 36 million individuals were predicted to have dementia in 2010, and 115 million are expected by 2050 [52]. One of the causes of AD is the aggregation and misfolding of beta-amyloid (Aβ) proteins, such as Aβ 40 or Aβ 42, which are thought to be toxic to neuronal cells [73]. Oxidative stress is another cause of AD [72]. Currently, there are no effective medications for AD [67].

Quercetin has a beneficial effect against neurological diseases such as AD [27]. Quercetin has been shown to reduce LPO, and neuronal cell death associated with AD environment [15]. Quercetin has low water solubility, which makes its use as a chemopreventive drug challenging when administered orally [50]. Low permeability, limited bioavailability (2%), substantial metabolism, hydrophobic nature, pH instability, and photodegradation are plausible factors contributing to the potential of quercetin [6].

Nanotechnology can be a critical strategy to overcome this problem by improving the bioavailability of a chemical and allowing it to target certain tissues [47]. Nanoparticles can penetrate both the mucosal barrier and blood–brain barrier to increase drug bioavailability through particle absorption [62]. Nanoscale alteration of materials can change their bioactivity and major features, such as solubility, circulation time, as well as accessibility to the target region [11]. Quercetin nanoparticles increased the relative oral bioavailability of quercetin by 523%, showing the possibility to decrease dosage using quercetin nanoparticles [8]. Nanoparticles ought to possess a size range of 1–100 nm, according to nanoscience principles [25]. The ideal size for passing through the blood–brain barrier is 20–100 nm. As a result, the smaller the size of the nanoparticles, the more effective the drug delivery [55].

The particle size of quercetin was reduced and made uniform using the antisolvent precipitation method. The precipitation method is a fast method for the synthesis of nanoparticles as well as a size-controllable method among the many chemical methods available [1]. TEM was used to investigate the structure of nanoparticles in this study. The results revealed that the quercetin nanoparticles were morphologically spherical and had uniform size distributions. The size range of quercetin nanoparticles was observed between 3.63–4.57 nm using the transmission electron microscope. DLS data revealed that quercetin nanoparticles formed nanoparticles with an average hydrodynamic diameter of 3.7 nm. This result is in agreement with the results obtained from the TEM images. From these results, we concluded that the particle size of quercetin nanoparticles produced by the antisolvent precipitation method was significantly small, which was more evident in the case of the sample prepared at a lower drug concentration (5 mg/ml), higher stirring speed (3000 rpm), and a higher solvent/antisolvent volume ratio of 1:40. The solvent-to-antisolvent ratio and stirring speed are important parameters that affect the particle size, and increasing these values reduces the particle size of quercetin to 3.7 nm. These findings corroborate previous findings, which indicated that decreasing the drug concentration, increasing the stirring speed, and increasing the solvent/antisolvent volume ratio favoured particle diameter reduction. The diameter of the quercetin particles was measured at 220 nm with a volume ratio of 1:25 [37]. In another study, the solvent/antisolvent volume ratio was reduced to 1:10 and the particle diameter was increased to 486 nm [1].

Histopathological studies of the hippocampus of acrolein-treated group revealed that acrolein induced distinct histological abnormalities affecting the CA1, CA2, CA3, and DG. The stratum pyramidale thickness in the CA1 and CA2 regions of the hippocampus was significantly reduced, with increased apoptotic neurones and dystrophic changes in the form of shrunken and irregular hyperchromatic and chromatolysis. The CA3 showed a decreased the stratum pyramidale thickness, as well as a considerable degree of atrophic ischaemic damage to the

(See figure on next page.)

Fig. 12 Electron micrograph of the microglia **a** Control group showing a dark elongated N with clumped chromatin and dark cytoplasm and long stretches rER. **b** Acrolein-treated group showing shrunken and completely damaged microglia with pyknotic N, degraded chromatin material and nucleoli, and nuclear membrane distortion. **c** Quercetin nanoparticle-treated group showing normal microglia. **d** Ameliorative group showing a dark elongated N with clumped chromatin and dark cytoplasm. **e** Protective group showing normal N with clumped chromatin and dark cytoplasm. **f** Recovery group showing irregular N with condensed chromatin. (N, nucleus; rER, rough endoplasmic reticulum). X 10000

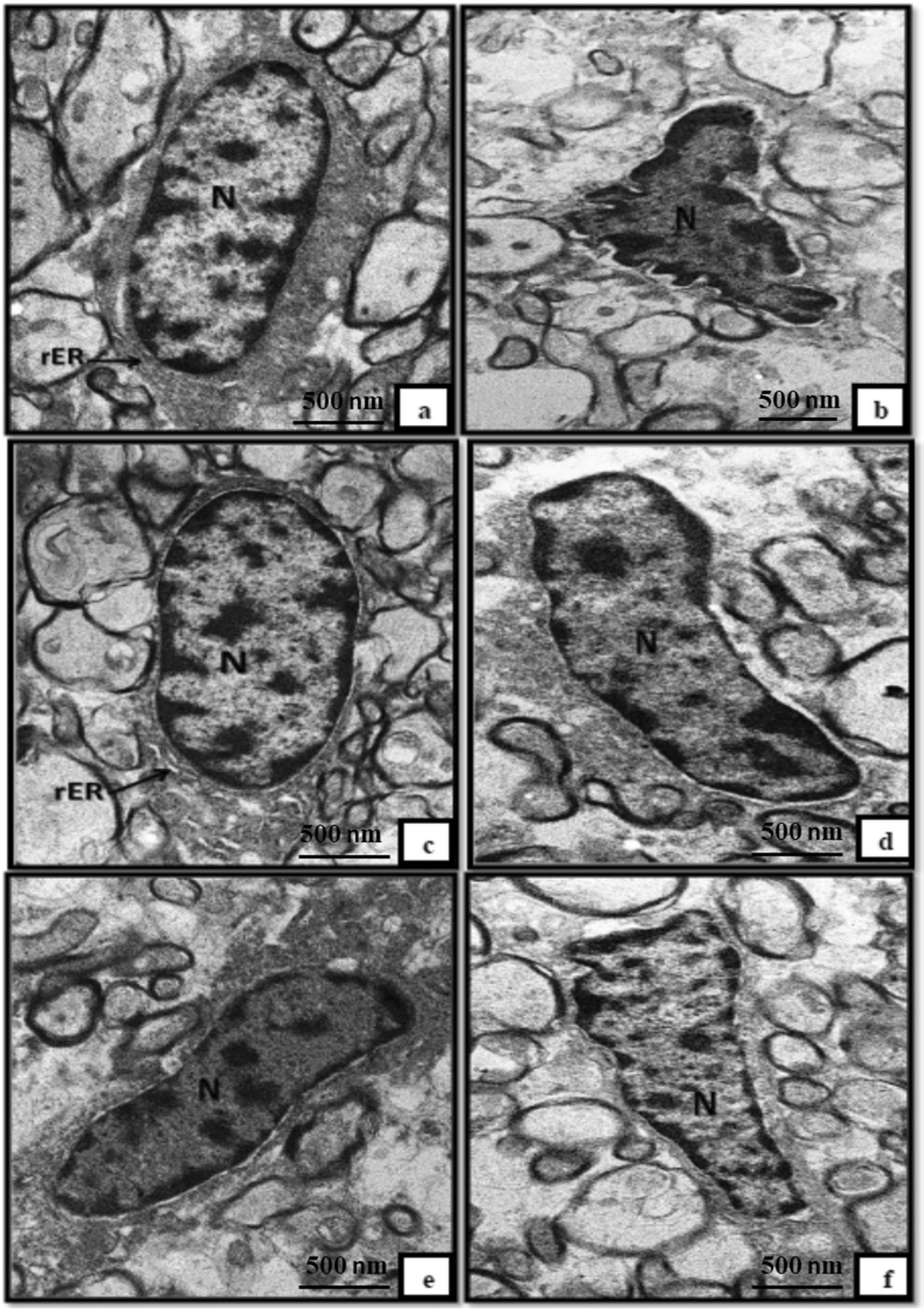

Fig. 12 (See legend on previous page.)

stratum pyramidale layer's neuronal cells, as well as neuronophagia. Acrolein caused atrophic ischaemia in the granular cells of the granular layer. Comparable results were reported by [76], who found that acrolein caused many histological abnormalities in brain tissues. [32] also found that acrolein caused pyknosis in rat hippocampal neurones. Pyknosis, which meaning irreversible condensation of the nucleus, has traditionally been applied as a marker of cell death [19]. Furthermore, acrolein has been linked to oxidative stress, protein aggregation, and cell death [18].

According to [14], Acrolein-induced neurotoxicity has been associated with cell death mechanisms, such as necrosis and apoptosis. Acrolein is an LPO byproduct and catalyst. LPO is the oxidation of polyunsaturated fatty acids in cells, caused by free radicals. [24]. The mechanism by which acrolein causes oxidative damage and neurotoxicity indicated in acrolein primarily involves binding and depletion of cellular nucleophiles, such as reduced glutathione (GSH). Acrolein causes the loss of antioxidants such as GSH and Superoxide dismutase, as well as an increase in ROS generation [46, 66]. The toxicity of acrolein has been linked to its extremely electrophilic character, which makes it easier for it to react with cellular compartments [40]. [14] reported that acrolein administered to Wistar rats for 8 weeks. This results in an increase in LPO, a decrease in reduced glutathione, and a reduction in total reduced thiol content, leading to an alteration of the central nervous system-associated behavioural patterns.

In the current study, quercetin nanoparticles showed significant improvement and were found to counteract the degenerative effects of acrolein administration. The histological abnormalities at several hippocampal sites improved dramatically in both the ameliorative and protective-treated groups. The CA1, CA2, and CA3 hippocampal parts of the ameliorative and protective groups showed a decrease in ischaemia neuronal injury of the stratum pyramidale layer's neuronal cells as well as an increase in stratum pyramidale layer thickness. Ischaemia neuronal damage within the granular cells of the granular layer was reduced in the DG hippocampus in the ameliorative and protective treatment groups. These results agree with those of [22], who reported that the administration of quercetin nanoparticles protected brain cells from arsenic-induced damage. [65] demonstrated that quercetin nanoparticles that target the blood–brain barrier while also protecting neurones from amyloid-beta fibrillation in a thioflavin T binding experiment were an effective method of quercetin administration and a potential technique for future AD treatments. The use of quercetin nanoparticles, which prevent oxidative damage and restore normal cellular function, is an excellent way to improve the cellular antioxidant defence system [8]. [64] stated that quercetin nanoparticles provide a preventative approach against the development of AD. Quercetin nanoparticles outperformed the quercetin-treated group of rats in terms of efficacy, suggesting that the improved efficacy is attributable to a longer residence period in systemic circulation and greater bioavailability. Quercetin nanoparticles significantly reduced malondialdehyde and acetylcholinesterase levels while increasing brain catalase and glutathione (GSH) levels [60]. reported that quercetin nanoparticles improve the oxidation of brain by increasing antioxidant enzyme activity and reducing pro-oxidant effects. Quercetin nanoparticles reduce reactive oxygen species (ROS), protein carbonyl, and myeloperoxidase. In addition, they increase the activities of glutathione peroxidase and acetylcholine esterase. [20] demonstrated that quercetin nanoparticles increased superoxide dismutase activity and GSH levels and reduced LPO. This finding revealed that enhanced antioxidant enzyme activity can lead to decreased intracellular H_2O_2 generation, which, when combined with an increase in GSH levels, can reduce LPO, suggesting that quercetin nanoparticles have significant antioxidant properties [15]. found that quercetin nanoparticles significantly increased memory retention. Furthermore, the persistence of LPO, glutathione, and nitrite levels confirmed that quercetin nanoparticles effectively target the central nervous system.

According to the morphometric analysis obtained in the present study, acrolein caused a great decrease in the number of normal pyramidal neurones, cell body diameter of pyramidal cells, and thickness of the pyramidal layer, as well as a decrease in the number of normal

(See figure on next page.)

Fig. 13 Electron micrograph of the neuron myelination (myelin sheath) **a** Control group showing a normal myelin sheath which is thick, electron-dense, and tightly wrapped around axonal cytoplasmic membranes. The myelinated axons had a smooth, regular contour. **b** Acrolein-treated group showing myelin sheath degeneration, localised disruption of another myelin sheath, and axoplasm vacuolation. **c** Quercetin nanoparticle-treated group exhibited a typical myelin sheath. **d** Ameliorative group showing preservation of the myelin sheath, except for a few axons. **e** Protective group showing great preservation of the myelin sheath, except for very few axons. **f** Recovery group showing myelin sheath degradation, axoplasm vacuolation, and localised rupture of another myelin sheath. (M, myelin sheath; X, axoplasm; V, vacuole; arrows, focal interruption of myelin sheath). X 20000

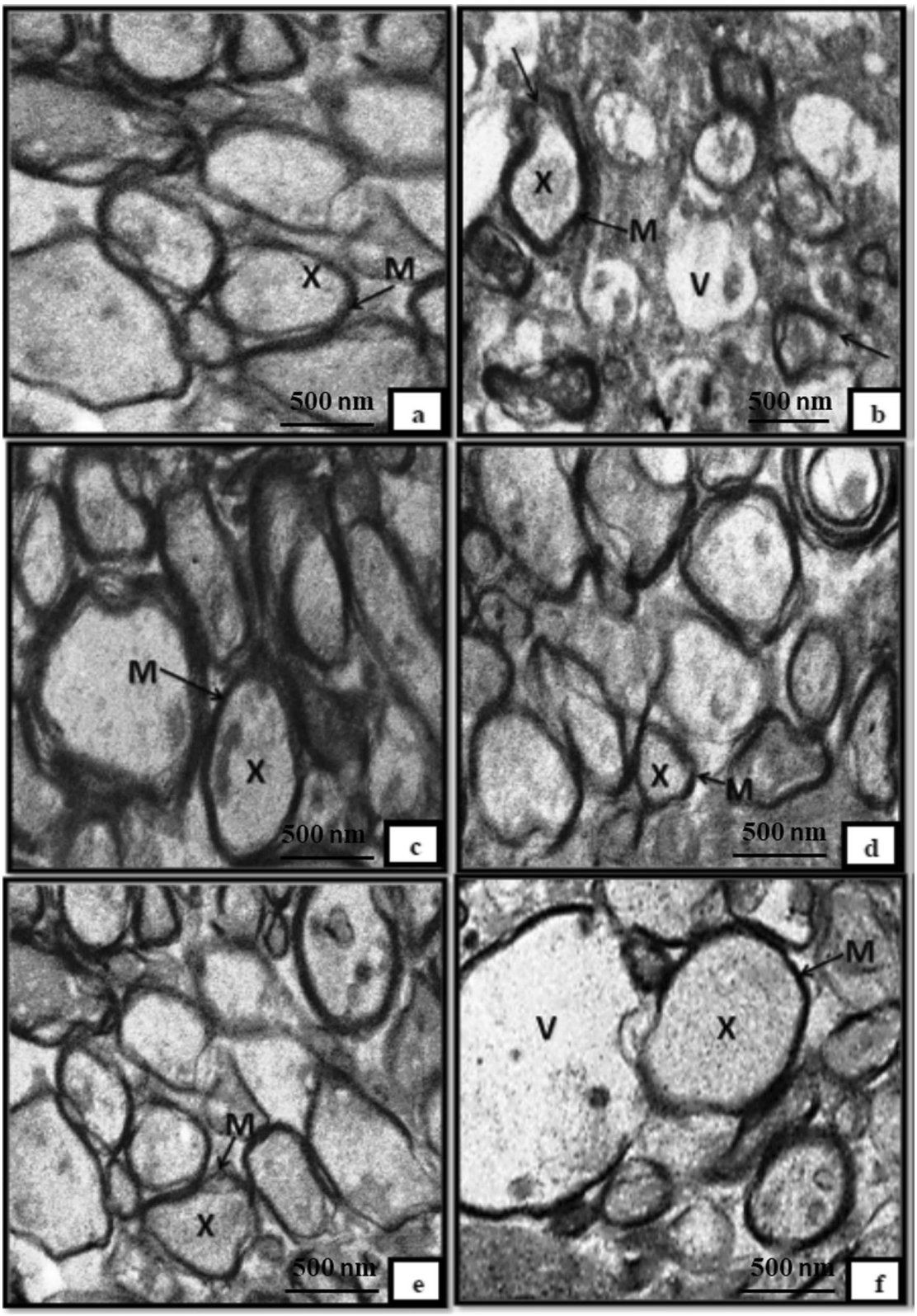

Fig. 13 (See legend on previous page.)

granular neurones, cell body diameter of the granular cells, and the granular layer thickness in the DG region. The current study found that in the case of treatment with quercetin nanoparticles in both the ameliorative and protective treatment groups, there was a great increase in the number of normal pyramidal neurones, the cell body diameter of the pyramidal cells, and the thickness of the pyramidal layer, as well as an increase in the number of normal granular neurones, the cell body diameter of granular cells, and the pyramidal layer thickness.

Multiple pathological lesions were observed in the hippocampus of acrolein-treated group. Semi-quantitative analysis of neuronal histopathological lesions in the acrolein-treated group indicated severe cellular oedema, ischaemic injury, malacia, gliosis, and the extent of lesions. However, treatment with quercetin nanoparticles has reversed these acrolein-induced morphological aberrations. This could be attributed to the antioxidant properties of quercetin nanoparticles or the combined anti-inflammatory and antioxidant roles of quercetin nanoparticles in neurotoxicity, as documented in previous studies [7].

The ultrastructure studies on the hippocampus treated with acrolein revealed that acrolein can induce cytotoxic effects in the nerve cells of the hippocampus. Acrolein causes significant distortion of the cellular structure of the hippocampus. [2] reported that acrolein causes neurotoxicity in hippocampal cells, primary cortical neurones, and dorsal root ganglionic neurones, revealing a key role for acrolein toxicity in neurodegeneration. Ultrastructural images of the pyramidal neurones indicated severe damage in the pyramidal neurones, which was confirmed by the pyknotic nuclei, degraded chromatin material, nuclear membrane deformations, and the presence of empty vacuolar structures. This damage could be related to the fact that acrolein causes damage to the nuclei of neurones by activating ROS generation and LPO [16]. Among all brain areas, pyramidal neurones in the hippocampus are most susceptible to ROS causing ischaemia damage and neuronal cell death [33]. Pyramidal cell death is distinguished by a selective neuronal loss that occurs over a 24–72-h process known as delayed neuronal death [23].

Vacuolation observed in pyramidal neurones has been explained by some researchers because of significant disruptions in lipid inclusions. Some researchers hypothesised that vacuolation was caused by cell damage, which increased the generation of ROS, destroyed the membranes, and changed their permeability [45]. Other researchers have emphasised that LPO is an autocatalytic mechanism that leads to the oxidative degradation of cellular membranes [31, 60]. Administration of quercetin nanoparticles resulted in a great improvement in the ultrastructure of the hippocampal pyramidal cells in the ameliorated and protective groups of rats. These improvements were observed in the presence of normal pyramidal neurones, which had large, rounded nucleus and well-developed organoids.

The ultrastructure of astrocytes in the hippocampus from the acrolein-treated group showed substantial damage, as was seen by a bloated nucleus with little heterochromatin clumping at the nuclear periphery. The severely injured cytoplasm was empty, with a few scattered damaged cellular organelles such as mitochondria. These results agree with those of a previous study [33], which found that acrolein causes mitochondrial damage in hippocampus cells, which leads to neuronal death. Mitochondrial damage has been found in AD brain tissue [53]. According to [5], astrocytes play a critical role in maintaining neurovascular unit homoeostasis by uptaking glutamate. Quercetin nanoparticles were found to have both ameliorative and protective effects against injury caused by acrolein on the ultrastructure of astrocytes in the hippocampus. This was clear in the nuclei of astrocytes, which were normal. Several organelles in astrocytes appeared normal. These results are consistent with the findings of [70], who demonstrated that quercetin nanoparticles preserve the ultrastructure and function of hippocampal astrocytes and regulate astrocyte activity.

Astrocytes may produce interleukin-33, which promotes engulfment of microglial synapses and development of neural circuits [21]. Astrogliosis develops in response to brain damage and Aβ accumulation, is triggered by inflammatory mediators, and has been linked to the neurodegenerative disease AD [77]. Astrogliosis may be a protective mechanism in AD, as astrocytes can remove Aβ and reduce the formation of amyloid plaques [39].

The ultrastructure of microglial cells in the hippocampus from the acrolein-treated group showed shrunken and fully destroyed microglia with pyknotic nuclei. These findings are consistent with [9, 76], who reported that acrolein induces shrinkage of the cell nucleus/pyknosis and loss of cytoplasm in the rat brain. According to [69, 74], microglial cells are central nervous system-resident macrophages.

In both the ameliorative and protective treatment groups, quercetin nanoparticles were shown to have a significant positive effect on the ultrastructure of hippocampal microglia, which was indicated by the presence of normal microglia after treatment with these nanoparticles. This is consistent with the conclusions reached by [28, 29], who reported that the quercetin nanoparticle-treated group showed a predominance of normal microglia with only a few dark microglia. This could be

the ability of quercetin nanoparticles to prevent oxidative stress, neuroinflammation, and amyloid plaques formation.

Acrolein's deteriorating effects extended to extra-neuronal structures such as nerve axons and myelin sheaths. The ultrastructural changes in neuron myelination in the acrolein-treated group revealed myelin damage and axonal degeneration. These results agree with those of [18], who proposed that acrolein caused myelin damage and that it was involved in the aetiology of multiple sclerosis [13] showed that oxidative stress caused by acrolein is a major cause of myelin damage. Acrolein can cause direct damage to myelin. [34, 38] reported that acrolein directly causes axonal damage. According to [32] who reported that acrolein, when combined, has the potential to damage axons via both direct and indirect mechanisms. [24] reported that acrolein induces axonal degeneration, demyelination, and macrophage infiltration [18] found that acrolein-induced oxidative stress and pro-inflammatory cytokines cause pathological damage to nerve tissues. The axons of the acrolein-treated group of myelinated nerve fibres were enlarged, oedematous, central, and degraded.

According to [10], myelin damage occurs when acrolein interacts directly with myelin basic protein. Owing to its lipid content, acrolein has been linked to axonal damage, and axons have been identified as a potential target for acrolein assault under oxidative stress [13]. Increased acrolein levels have been linked to neuronal membrane damage, loss of conduction, and neuronal degeneration [49]. Axon alterations are part of a neuronal injury, whereas myelination is disrupted by changes in myelin basic protein [3]. Demyelination can develop because of axonal degeneration or oxidative stress [4].

Axonal damage is linked to Aβ accumulation and tau hyperphosphorylation and may play a role in AD-related neuronal communication problems [29]. Indeed, axonal damage inhibits axonal transport, leading to total transport obstruction, axonal leakage, synaptic dysfunction, and axonal degeneration over time [44]. Axonal damage is associated with retrograde neuronal apoptosis [61]. According to [63], acrolein causes myelin sheath degradation in addition to axonal damage.

Quercetin nanoparticles were also found to have ameliorative and protective effects against acrolein injury in the hippocampal myelin sheath and axons, and this was confirmed by the preservation of the myelin sheath. These results are in agreement with those of [70] who found that the administration of quercetin nanoparticles nearly eliminated the formation of acrolein-induced amyloid plaques and neurofibrillary tangles, preserving axons, myelin sheaths, and synaptic structures. This significant finding can be explained by quercetin's multifaceted nature, which makes it more effective when applied as a nanoparticle [22].

5 Conclusions

Acrolein has been proven to induce histopathological and ultrastructural alterations in the hippocampus. Therefore, controlling acrolein in the environment is important for health. Quercetin nanoparticles have been found to significantly reduce the potential of abnormal toxic lesions induced by acrolein in the hippocampus, and they are recommended for use in nanomedicine to protect and improve nervous tissues. Quercetin nanoparticles provide insights into potential therapies for preventing AD after oxidative stress induced by acrolein.

Abbreviations

AD	Alzheimer's disease
TEM	Transmission electron microscopy
DLS	Dynamic light scattering
CA1	Cornu ammonis 1
CA2	Cornu ammonis 2
CA3	Cornu ammonis 3
DG	Dentate gyrus
S	Subiculum
TDI	Tolerable Daily Intake
Aβ	Beta-amyloid
GSH	Reduced glutathione
ROS	Reactive oxygen species
LPO	Lipid peroxidation

Acknowledgements

Not applicable.

Author contributions

All authors participated in the study conceptualisation, and design of the studies. RF conducted experiments, conducted the study, and drafted the manuscript. SMS and SN reviewed the manuscript.

Funding

The authors received no financial support for this article's research, authorship, and/or publication.

Availability of data and materials

The datasets used in this study are available upon reasonable request from the corresponding author.

Declarations

Ethics approval and consent to participate

The current experimental design was examined and authorised by the research ethical committee of Zagazig University, Egypt (approval number Zu-IACUC/1/F/306).

Consent for publication

Not applicable.

Competing interests

The authors declared no potential conflicts of interest concerning this article's research, authorship, and/or publication.

Received: 10 July 2023 Accepted: 5 January 2024
Published online: 15 January 2024

References

1. Abd El-Rahmanand SN, Suhailah S (2014) Quercetin nanoparticles: preparation and characterization. Indian J Drugs 2:96–103
2. Abraham K, Andres S, Palavinskas R, Berg K, Appel KE, Lampen A (2011) Toxicology and risk assessment of acrolein in food. Mol Nutr Food Res 55:1277–1290
3. Afifi OK, Embaby AS (2016) Histological study on the protective role of ascorbic acid on cadmium-induced cerebral cortical neurotoxicity in adult male albino rats. J Microsc Ultrastruct 4:36–45
4. Alizadeh A, Dyck SM, Karimi-Abdolrezaee S (2015) Myelin damage and repair in pathologic CNS: challenges and prospects. Front Mol Neurosci 8:35
5. Anderson CM, Swanson RA (2000) Astrocyte glutamate transport: review of properties, regulation, and physiological functions. Glia 32:1–14
6. Aytac Z, Kusku SI, Durgun E, Uyar T (2016) Quercetin/β-cyclodextrin inclusion complex embedded nanofibres: slow release and high solubility. Food Chem 197:864–871
7. Batiha GE-S, Beshbishy AM, Ikram M, Mulla ZS, El-Hack MEA, Taha AE et al (2020) The pharmacological activity, biochemical properties, and pharmacokinetics of the major natural polyphenolic flavonoid: Quercetin. Foods 9:374
8. Birinci Y, Niazi JH, Aktay-Çetin O, Basaga H (2020) Quercetin in the form of a nano-antioxidant (QTiO2) provides stabilization of quercetin and maximizes its antioxidant capacity in the mouse fibroblast model. Enzyme Microb Technol 138:109559
9. Bisht K, Sharma KP, Lecours C, Gabriela Sánchez M, El Hajj H, Milior G et al (2016) Dark microglia: a new phenotype predominantly associated with pathological states. Glia 64:826–839
10. Boggs J (2006) Myelin basic protein: a multifunctional protein. Cell Mol Life Sci CMLS 63:1945–1961
11. Caruthers SD, Wickline SA, Lanza GM (2007) Nanotechnological applications in medicine. Curr Opin Biotechnol 18:26–30
12. Chen B-Q, Zhao Y, Zhang Y, Pan Y-J, Xia H-Y, Kankala RK et al (2023) Immune-regulating camouflaged nanoplatforms: a promising strategy to improve cancer nano-immunotherapy. Bioactive Mater 21:1–19
13. Chen C, Lu J, Peng W, Mak MS, Yang Y, Zhu Z et al (2022) Acrolein, an endogenous aldehyde induces Alzheimer's disease-like pathologies in mice: a new sporadic AD animal model. Pharmacol Res 175:106003
14. da Silva BL, Schnorr CE, Santos DC, Rostirolla DC, Moresco KS, Ozório P et al (2020) Chronic acrolein exposure in Wistar rats: the effects of guarana extracts. J Funct Foods 65:103733
15. Dhawan S, Kapil R, Singh B (2011) Formulation development and systematic optimization of solid lipid nanoparticles of quercetin for improved brain delivery. J Pharm Pharmacol 63:342–351
16. Ebokaiwe AP, Ushang OR, Ogunwa TH, Kikiowo B, Olusanya O (2022) Quercetin attenuates cyclophosphamide induced-immunosuppressive indoleamine 2, 3-dioxygenase in the hippocampus and cerebral cortex of male Wister rats. J Biochem Mol Toxicol 36:e23179
17. El-Maghrabey MH, El-Shaheny R, El Hamd MA, Al-Khateeb LA, Kishikawa N, Kuroda N (2022) Aldehydes' sources, toxicity, environmental analysis, and control in food. In: Organic pollutants: toxicity and solutions, pp 117–151
18. Erhan E, Salcan I, Bayram R, Suleyman B, Dilber M, Yazici GN et al (2021) Protective effect of lutein against acrolein-induced ototoxicity in rats. Biomed Pharmacother 137:111281
19. Fujikawa DG, Zhao S, Ke X, Shinmei SS, Allen SG (2010) Mild as well as severe insults produce necrotic, not apoptotic, cells: evidence from 60-min seizures. Neurosci Lett 469:333–337
20. Ghaffari F, Moghaddam AH, Zare M (2018) Neuroprotective effect of quercetin nanocrystal in a 6-hydroxydopamine model of Parkinson disease: biochemical and behavioural evidence. Basic Clin Neurosci 9:317
21. Ghoneim FM, Khalaf HA, Elsamanoudy AZ, El-Khair SMA, Helaly AM, Mahmoud E-HM et al (2015) Protective effect of chronic caffeine intake on gene expression of brain-derived neurotrophic factor signalling and the immunoreactivity of glial fibrillary acidic protein and Ki-67 in Alzheimer's disease. Int J Clin Exp Pathol 8:7710
22. Ghosh A, Mandal AK, Sarkar S, Panda S, Das N (2009) Nanoencapsulation of quercetin enhances its dietary efficacy in combating arsenic-induced oxidative damage in the liver and brain of rats. Life Sci 84:75–80
23. Ghosh A, Sarkar S, Mandal AK, Das N (2013) Neuroprotective role of nano encapsulated quercetin in combating ischemia-reperfusion induced neuronal damage in young and aged rats. PLoS ONE 8:e57735
24. Gianaris A, Liu N-K, Wang X-F, Oakes E, Brenia J, Gianaris T et al (2016) Unilateral microinjection of acrolein into thoracic spinal cord produces acute and chronic injury and functional deficits. Neuroscience 326:84–94
25. Gigault J, El Hadri H, Nguyen B, Grassl B, Rowenczyk L, Tufenkji N et al (2021) Nanoplastics are neither microplastics nor engineered nanoparticles. Nat Nanotechnol 16:501–507
26. Goma AA, El Okle OS, Tohamy HG (2021) Protective effect of methylene blue against copper oxide nanoparticle-induced neurobehavioral toxicity. Behav Brain Res 398:112942
27. Grewal AK, Singh TG, Sharma D, Sharma V, Singh M, Rahman MH et al (2021) Mechanistic insights and perspectives involved in neuroprotective action of quercetin. Biomed Pharmacother 140:111729
28. Hayden MR, Grant DG, Aroor AR, DeMarco VG (2018) Ultrastructural remodelling of the neurovascular unit in the female diabetic db/db model–part II: microglia and mitochondria. Neuroglia 1:311–326
29. Hellwig K, Kvartsberg H, Portelius E, Andreasson U, Oberstein TJ, Lewczuk P et al (2015) Neurogranin and YKL-40: independent markers of synaptic degeneration and neuroinflammation in Alzheimer's disease. Alzheimer's Res Therapy 7:1–8
30. Henning RJ, Johnson GT, Coyle JP, Harbison RD (2017) Acrolein can cause cardiovascular disease: a review. Cardiovasc Toxicol 17:227–236
31. Hernández-Cruz EY, Amador-Martínez I, Aranda-Rivera AK, Cruz-Gregorio A, Chaverri JP (2022) Renal damage induced by cadmium and its possible therapy by mitochondrial transplantation. Chem Biol Interact 361:109961
32. Huang Y-J, Jin M-H, Pi R-B, Zhang J-J, Ouyang Y, Chao X-J et al (2013) Acrolein induces Alzheimer's disease-like pathologies in vitro and in vivo. Toxicol Lett 217:184–191
33. Huang Y, Qin J, Chen M, Chao X, Chen Z, Ramaswamy C et al (2014) Lithium prevents acrolein-induced neurotoxicity in HT22 mouse hippocampal cells. Neurochem Res 39:677–684
34. Iyer AM, Dadlani V, Pawar HA (2022) Review on acrylamide: a hidden hazard in fried carbohydrate-rich food. Curr Nutr Food Sci 18:274–286
35. Jiménez-Morales JM, Hernández-Cuenca YE, Reyes-Abrahantes A, Ruiz-García H, Barajas-Olmos F, García-Ortiz H et al (2022) MicroRNA delivery systems in glioma therapy and perspectives: a systematic review. J Control Release 349:712–730
36. Jing M, Jiang Q, Zhu Y, Fan D, Wang M, Zhao Y (2022) Effect of acrolein, a lipid oxidation product, on the formation of the heterocyclic aromatic amine 2-amino-1-methyl-6-phenylimidazo [4, 5-b] pyridine (PhIP) in model systems and roasted tilapia fish patties. Food Chem X 14:100315
37. Kakran M, Sahoo NG, Li L, Judeh Z (2012) Fabrication of quercetin nanoparticles by anti-solvent precipitation method for enhanced dissolution. Powder Technol 223:59–64
38. Kalafatakis I, Savvaki M, Velona T, Karagogeos D (2021) Implication of contactins in demyelinating pathologies. Life 11:51
39. Kaur D, Sharma V, Deshmukh R (2019) Activation of microglia and astrocytes: a roadway to neuroinflammation and Alzheimer's disease. Inflammopharmacology 27:663–677
40. Kehrer JP, Biswal SS (2000) The molecular effects of acrolein. Toxicol Sci 57:6–15
41. Khammash D, Rajagopal SK, Polk TA (2023) The neurobiology of ageing. In: Neurobiology of brain disorders, 977–993
42. Khoramjouy M, Naderi N, Kobarfard F, Heidarli E, Faizi M (2021) An intensified acrolein exposure can affect memory and cognition in rats. Neurotox Res 39:277–291
43. Kobori M, Takahashi Y, Sakurai M, Akimoto Y, Tsushida T, Oike H et al (2016) Quercetin suppresses immune cell accumulation and improves mitochondrial gene expression in adipose tissue of diet-induced obese mice. Mol Nutr Food Res 60:300–312
44. Krstic D, Knuesel I (2013) Deciphering the mechanism underlying late-onset Alzheimer's disease. Nat Rev Neurol 9:25–34
45. Krukowski K, Nolan A, Becker M, Picard K, Vernoux N, Frias ES et al (2021) Novel microglia-mediated mechanisms underlying synaptic loss and

cognitive impairment after traumatic brain injury. Brain Behav Immunity 98:122–135
46. Kumar M, Bansal N (2022) A revisit to etiopathogenesis and therapeutic strategies in Alzheimer's disease. Curr Drug Targets 23:486–512
47. Kuo Y-C, Chou P-R (2014) Neuroprotection against degeneration of SK-N-MC cells using neuron growth factor-encapsulated liposomes with the surface report and transferrin. J Pharm Sci 103:2484–2497
48. Lai F, Franceschini I, Corrias F, Sala MC, Cilurzo F, Sinico C et al (2015) Maltodextrin fast dissolving films for quercetin nanocrystal delivery. A feasibility study. Carbohydr Polym 121:217–223
49. Leung G, Sun W, Zheng L, Brookes S, Tully M, Shi R (2011) Anti-acrolein treatment improves behavioural outcome and alleviates myelin damage in experimental autoimmune encephalomyelitis mouse. Neuroscience 173:150–155
50. Li H, Zhao X, Ma Y, Zhai G, Li L, Lou H (2009) Enhancement of gastrointestinal absorption of quercetin by solid lipid nanoparticles. J Control Release 133:238–244
51. Li Z, Deng H, Guo X, Yan S, Lu C, Zhao Z et al (2022) Effective dose/duration of natural flavonoid quercetin for treatment of diabetic nephropathy: a systematic review and meta-analysis of rodent data. Phytomedicine 154348.
52. Luo C-l, Liu Y-q, Wang P, Song C-h, Wang K-j, Dai L-p et al (2016) The effect of quercetin nanoparticle on cervical cancer progression by inducing apoptosis, autophagy and anti-proliferation via JAK2 suppression. Biomed Pharmacother 82:595–605
53. Maczurek A, Hager K, Kenklies M, Sharman M, Martins R, Engel J et al (2008) Lipoic acid as an anti-inflammatory and neuroprotective treatment for Alzheimer's disease. Adv Drug Deliv Rev 60:1463–1470
54. Masters CL, Bateman R, Blennow K, Rowe CC, Sperling RA, Cummings JL (2015) Alzheimer's disease. Nat Rev Dis Primers 1:1–18
55. Meng Q, Meng H, Pan Y, Liu J, Li J, Qi Y et al (2022) Influence of nanoparticle size on blood–brain barrier penetration and the accumulation of anti-seizure medicines in the brain. J Mater Chem B 10:271–281
56. Michala A-S, Pritsa A (2022) Quercetin: a molecule of great biochemical and clinical value and its beneficial effect on diabetes and cancer. Diseases 10:37
57. Millar PR, Luckett PH, Gordon BA, Benzinger TL, Schindler SE, Fagan AM et al (2022) Predicting brain age from functional connectivity in symptomatic and preclinical Alzheimer disease. Neuroimage 256:119228
58. Minaei A, Sabzichi M, Ramezani F, Hamishehkar H, Samadi N (2016) Co-delivery with nano-quercetin enhances doxorubicin-mediated cytotoxicity against MCF-7 cells. Mol Biol Rep 43:99–105
59. Mishra R, Kulkarni S (2022) A review of various pharmacological effects of quercetin with its barriers and approaches for solubility and permeability enhancement. Nat Prod J 12:9–21
60. Mohamed HK, Mohamed HZ-E-A (2018) A histological and immunohistochemical study on the possible protective role of silymarin on cerebellar cortex neurotoxicity of lactating albino rats and their pups induced by gibberellic acid during late pregnancy and early postnatal period. Egyptian Journal of Histology 41:345–371
61. Mori F, Tanji K, Yoshida Y, Wakabayashi K (2002) Thalamic retrograde degeneration in the congenitally hydrocephalic rat is attributable to apoptotic cell death. Neuropathology 22:186–193
62. Nahum V, Domb AJ (2022) Solid lipid microspheres decorated nanoparticles as drug carriers. Int J Pharm 621:121797
63. Nasrabady SE, Rizvi B, Goldman JE, Brickman AM (2018) White matter changes in Alzheimer's disease: a focus on myelin and oligodendrocytes. Acta Neuropathol Commun 6:1–10
64. Palle S, Neerati P (2017) Quercetin nanoparticles attenuate scopolamine-induced spatial memory deficits and pathological damages in rats. Bull Facul Pharm Cairo Univ 55:101–106
65. Pinheiro R, Granja A, Loureiro JA, Pereira M, Pinheiro M, Neves AR et al (2020) Quercetin lipid nanoparticles functionalized with transferrin for Alzheimer's disease. Eur J Pharm Sci 148:105314
66. Pocernich CB, Butterfield DA (2012) Elevation of glutathione as a therapeutic strategy in Alzheimer's disease. BBA-Mol Basis Dis 1822:625–630
67. Qin L-H, Wang C, Qin L-W, Liang Y-F, Wang G-H (2019) Spore powder of Ganoderma lucidum for Alzheimer's disease: a protocol for systematic review. Medicine 98
68. Rahman MM, Islam MR, Akash S, Harun-Or-Rashid M, Ray TK, Rahaman MS et al (2022) Recent advancements of nanoparticles application in cancer and neurodegenerative disorders: at a glance. Biomed Pharmacother 153:113305
69. Ries M, Sastre M (2016) Mechanisms of Aβ clearance and degradation by glial cells. Front Ageing Neurosci 8:160
70. Rifaai RA, Mokhemer SA, Saber EA, Abd El-Aleem SA, El-Tahawy NFG (2020) Neuroprotective effect of quercetin nanoparticles: a possible prophylactic and therapeutic role in Alzheimer's disease. J Chem Neuroanat 107:101795
71. Riphagen JM, Suresh MB, Salat DH, AsDN I (2022) The canonical pattern of Alzheimer's disease atrophy is linked to white matter hyperintensities in normal controls, differently in normal controls compared to in AD. Neurobiol Aging 114:105–112
72. Rummel NG, Butterfield DA (2022) Altered metabolism in Alzheimer disease brain: role of oxidative stress. Antioxid Redox Signal 36:1289–1305
73. Salahuddin P, Fatima MT, Uversky VN, Khan RH, Islam Z, Furkan M (2021) The role of amyloids in Alzheimer's and Parkinson's diseases. Int J Biol Macromol 190:44–55
74. Salter MW, Stevens B (2017) Microglia emerge as central players in brain disease. Nat Med 23:1018–1027
75. Savonenko AV, Wong PC, Li T (2023) Alzheimer diseases. Neurobiology of brain disorders. Elsevier, pp 313–336
76. Selmanoğlu G, Özgün GM, Karacaoğlu E (2018) Acrolein-mediated neurotoxicity in growing Wistar male rats. Pestic Biochem Physiol 149:37–43
77. Selvakumar K, Bavithra S, Krishnamoorthy G, Arunakaran J (2018) Impact of quercetin on tight junctional proteins and BDNF signalling molecules in the hippocampus of PCBs-exposed rats. Interdiscip Toxicol 11:294
78. Suvarna KS, Layton C, Bancroft JD (2018) Bancroft's theory and practice of histological techniques. Elsevier health sciences

Publisher's Note